Review of Scientific Instruments

Multispectral multidimensional spectrometer spanning the ultraviolet to the mid-infrared

Cite as: Rev. Sci. Instrum. **90**, 013108 (2019); https://doi.org/10.1063/1.5055244
Submitted: 06 September 2018 . Accepted: 29 November 2018 . Published Online: 24 January 2019

Yin Song, Arkaprabha Konar, Riley Sechrist, Ved Prakash Roy, Rong Duan, Jared Dziurgot, Veronica Policht, Yassel Acosta Matutes, Kevin J. Kubarych, and Jennifer P. Ogilvie

Review of Scientific Instruments ARTICLE scitation.org/journal/rsi

Multispectral multidimensional spectrometer spanning the ultraviolet to the mid-infrared

Cite as: Rev. Sci. Instrum. 90, 013108 (2019); doi: 10.1063/1.5055244
Submitted: 6 September 2018 • Accepted: 29 November 2018 •
Published Online: 24 January 2019

Yin Song,[1] Arkaprabha Konar,[1] Riley Sechrist,[1] Ved Prakash Roy,[2] Rong Duan,[2] Jared Dziurgot,[1] Veronica Policht,[1] Yassel Acosta Matutes,[1] Kevin J. Kubarych,[2] and Jennifer P. Ogilvie[1,a)]

AFFILIATIONS

[1] Department of Physics, University of Michigan, 450 Church St., Ann Arbor, Michigan 48109, USA
[2] Department of Chemistry, University of Michigan, 930 N University Ave., Ann Arbor, Michigan 48109, USA

[a)] **Author to whom correspondence should be addressed:** jogilvie@umich.edu

ABSTRACT

Multidimensional spectroscopy is the optical analog to nuclear magnetic resonance, probing dynamical processes with ultrafast time resolution. At optical frequencies, the technical challenges of multidimensional spectroscopy have hindered its progress until recently, where advances in laser sources and pulse-shaping have removed many obstacles to its implementation. Multidimensional spectroscopy in the visible and infrared (IR) regimes has already enabled respective advances in our understanding of photosynthesis and the structural rearrangements of liquid water. A frontier of ultrafast spectroscopy is to extend and combine multidimensional techniques and frequency ranges, which have been largely restricted to operating in the distinct visible or IR regimes. By employing two independent amplifiers seeded by a single oscillator, it is straightforward to span a wide range of time scales (femtoseconds to seconds), all of which are often relevant to the most important energy conversion and catalysis problems in chemistry, physics, and materials science. Complex condensed phase systems have optical transitions spanning the ultraviolet (UV) to the IR and exhibit dynamics relevant to function on time scales of femtoseconds to seconds and beyond. We describe the development of the Multispectral Multidimensional Nonlinear Spectrometer (MMDS) to enable studies of dynamical processes in atomic, molecular, and material systems spanning femtoseconds to seconds, from the UV to the IR regimes. The MMDS employs pulse-shaping methods to provide an easy-to-use instrument with an unprecedented spectral range that enables unique combination spectroscopies. We demonstrate the multispectral capabilities of the MMDS on several model systems.

INTRODUCTION

Multidimensional optical spectroscopy is the optical analog to nuclear magnetic resonance (NMR), probing dynamical processes with ultrafast (10^{-15}–10^{-12} s) time resolution. Correlating the excitation and detection frequencies of a physical system through the nonlinear optical response allows direct access to spectral features and to dynamics that are obscured in conventional one-dimensional spectra.[1] A 2D spectrum can be thought of as pump-probe transient absorption with equal spectral resolution of both the pump and the probe (Fig. 1) and is therefore a map correlating excitation and detection frequencies.[2–10] At optical frequencies, technical challenges have hindered progress until relatively recently, when advances in laser sources and pulse-shaping are removing obstacles. In the past ~20 years, multidimensional spectroscopy in the visible and infrared (IR) regimes has enabled novel measurements of challenging condensed phase systems ranging from quantum wells and liquids to proteins and catalysts.[11–19] Phenomena ranging from protein folding and photosynthesis to charge transport and photocatalysis exhibit relevant energetic and dynamical changes on time scales from femtoseconds to seconds. One of the great open challenges in understanding complex, multi-tiered dynamical systems is to understand what links seemingly distinct length and time scales. To meet these challenges, the next generation of ultrafast spectroscopy must extend the temporal observation window and combine multidimensional techniques and frequency ranges. We report

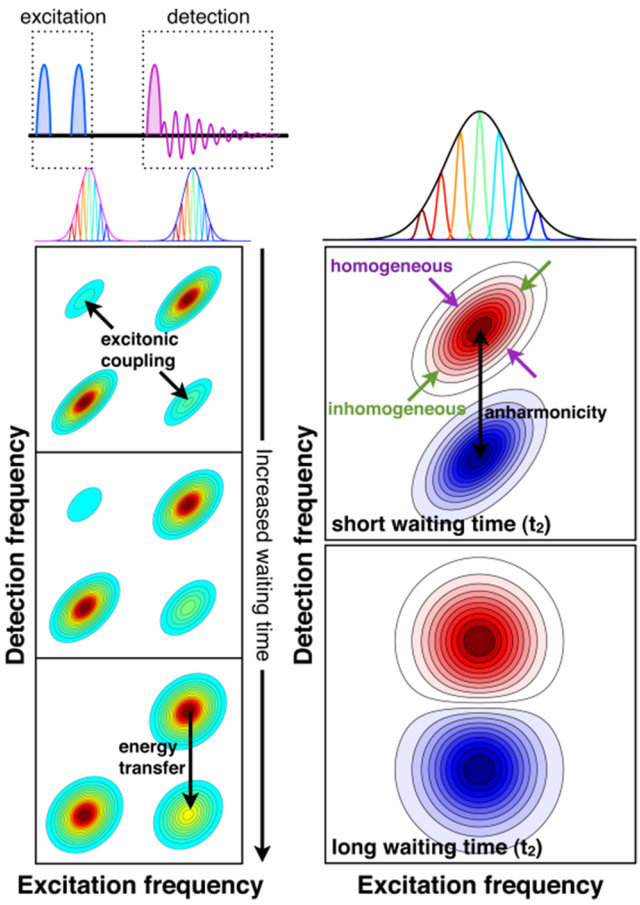

FIG. 1. Pulse sequence (top) and schematic 2D spectra (left) showing correlated 2D line shapes reflecting inhomogeneity hidden in the 1D absorption spectrum, anharmonicity, and lineshape evolution with increased waiting time due to spectral diffusion. (Right) Coupled excitonic systems typical of multichromophoric aggregates and light harvesting complexes, highlighting coupling, inhomogeneous broadening, energy transfer, and spectral diffusion.

the development of a general multispectral multidimensional spectrometer (the "MMDS") capable of accessing transitions from the ultraviolet (UV) to the infrared to enable breakthrough structural and dynamical characterization of next generation condensed phase systems.

Construction of the 2D frequency map requires multiple field interactions with control over either the relative timing between pulses or over center frequency of the excitation pulse. The basic pulse sequence for two-color 2D Fourier transform spectroscopy, as well as 2DUV with tunable narrowband excitation, is shown in Fig. 2, along with the general layout of the MMDS. The most popular implementation of 2D optical spectroscopy uses a pair of pulses separated by a time delay τ (often denoted the "coherence" time), followed by a third pulse delayed by T relative to the second pulse. The second time period is often called the "waiting" time. The signal field emitted by the macroscopic polarization induced in the sample by the three excitation pulses is detected by interference with a reference local oscillator field. In the case where the first two excitation pulses are collinear, the signal is emitted in the same direction as the third (i.e., "probe") pulse, which serves as the local oscillator.[20–26] In an alternative geometry, all three beams are non-collinear, and a fourth field must be provided for interference with the signal. The signal and local oscillator are typically detected in a spectrograph equipped with an array detector, providing the detection frequency directly. By varying the coherence time, the detected signal field will oscillate slightly differently at each detected pixel, and Fourier transforming the signal on each pixel with respect to τ results in a two-dimensional spectrum. Multiple 2D spectra are recorded at different waiting times (T) by stepping the delay between the second and third pulses.[5,9]

Multidimensional spectroscopy is an emerging field, but the technical difficulties of its implementation have limited its use to a small number of labs worldwide, studying a restricted set of scientific problems. Significant progress has recently been made toward simplifying the experimental implementation through the use of pulse-shaping. These advances and recent developments in broadband femtosecond pulse generation provide the opportunity to develop a truly unique easy-to-use instrument to enable multidimensional spectroscopy spanning the UV-IR, with unprecedented combination spectroscopies. The MMDS makes exclusive use of optical pulse shapers to implement the multidimensional pulse sequences in the pump probe geometry. An optical pulse shaper acts as a programmable linear filter, which can alter the spectral phase of a light field with accuracy that exceeds the requirements of 2D spectroscopy.[21–23,25–29]

There are several key advantages of using pulse shapers to produce the pulse sequences used in 2D spectroscopy. Since the first two pulses are collinear, one adopts the pump-probe geometry, where the signal propagates collinearly with the probe. In this geometry, the relative phase between the signal and the local oscillator (which is the probe) is well-defined and locked such that the recorded signal corresponds directly to the pump-induced change in absorption. The pump-probe geometry avoids the additional and often tricky step of "phasing" a 2D spectrum, a requirement for obtaining an absorptive spectrum in the noncollinear geometry. This implementation is easier to align and is compatible with multispectral experiments. With the pulse shaper's high phase fidelity, there is no appreciable uncertainty in the coherence time delay, eliminating the need to measure the first optical delay.

2D spectroscopy with a pulse-shaper also enables phase-cycling schemes—where multiple pulse pairs separated by the same envelope delay (i.e., linear phase) have different constant phases—that enable removal of scatter as well as the isolation of distinct dynamical pathways.[23,25,26,30,31] Scattering is a challenge in all coherent spectroscopy methods, but by shifting the frequency of the scattered signals outside of the measurement window, it is possible to suppress the background.[26,32] Any pair of pulses can interfere due to scattering, and combinations of phase cycling and chopping can significantly reduce contamination by scattering. Another key feature of phase-cycling is the ability to recover distinct Liouville space pathways, which can be helpful in interpreting

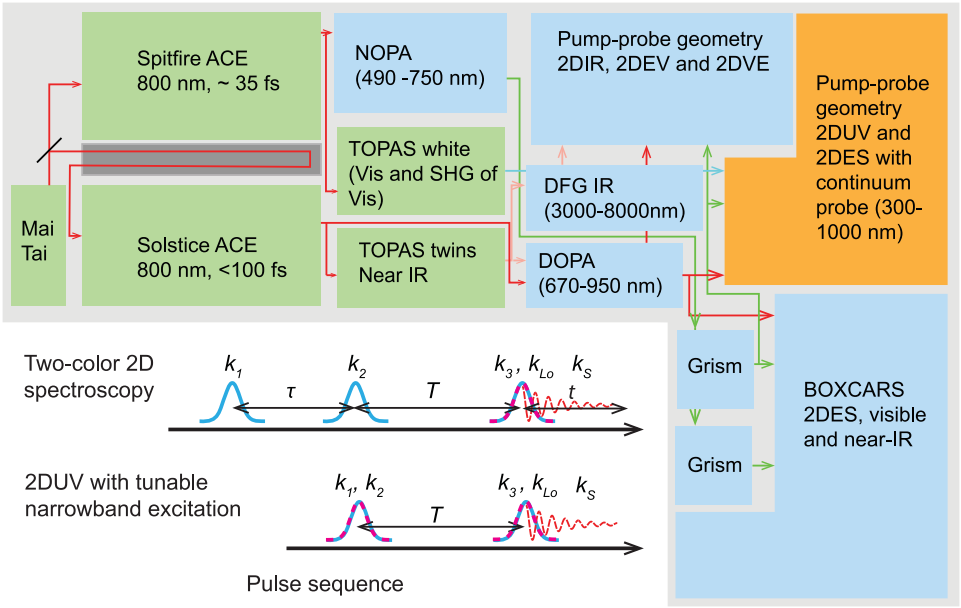

FIG. 2. Layout of the dual-amplifier multispectral multidimensional spectrometer (MMDS). The components combine commercial sources and specialized optics (such as pulse shapers) with homebuilt sources and experimental setups. Components are classified as (green) commercial, (blue) in-house developed using existing expertise of the co-PIs, and (orange) new technology that we will learn and develop. Arrows show that each wavelength range source can act either as a pump or a probe for multispectral multidimensional measurements or for transient 2D spectroscopy combining different spectral ranges. For 2DVE, the interference between the signal and the probe will be directed to the CCD camera of the pump-probe geometry 2DES setup for detection.

spectra and dynamics.[25] With non-collinear, background-free 2D spectroscopy, there are two signals that emerge with different wavevectors. By swapping the timing of the first two pulses, it is possible to record separately the so-called rephasing spectrum in the $k_- = -k_1 + k_2 + k_3$ direction and the non-rephasing spectrum in the $k_+ = +k_1 - k_2 + k_3$ direction.[33] Since the two signals report distinct dynamics—for example, there is no "echo" in the non-rephasing pathway—being able to decompose the purely absorptive spectrum into the rephasing and non-rephasing contributions actually increases the information content of the spectroscopy. Rephasing and non-rephasing contributions can readily be separated with phase-cycling.[25]

MULTISPECTRAL MULTIDIMENSIONAL SPECTROSCOPY

Figure 3(a) depicts an overview of the cutting-edge and conceivable multidimensional spectroscopies which are under development or will be developed in the near future. The whole family includes 2D ultraviolet (2DUV) spectroscopy, 2D electronic spectroscopy (2DES), 2D infrared (2DIR) spectroscopy, 2D terahertz (2DTHz) spectroscopy, as well as mixed-frequency 2D spectroscopy such as 2DEV, 2DVE, 2DTHz-ES, 2DTHz-IR, 2DIR-THz, and 2DE-THz. Multidimensional THz spectroscopy, which has been demonstrated by several groups,[34–37] is beyond the scope of the current work. In our manuscript, we will focus on the spectral range spanning from UV to mid-IR. One-color 2D electronic spectroscopy (2DES) and 2D infrared (2DIR) spectroscopy are mature techniques which have been implemented in many groups already. The frontier in multidimensional spectroscopy is to broaden the accessible range of measurable frequency correlations, whether using two-color methods or by continuum probe pulses.[23,25,38–55] The MMDS is designed to combine distinct spectral regions in order to leverage the powerful correlation of 2D spectroscopy, uncovering hidden structure in distinct spectral bands [Fig. 3(b)]. For each pair of frequency regions, there are two basic pulse sequences defined by the arrival order of the two "colors." For example, pumping with UV, visible, or near-IR excites electrons which then undergo excited state dynamics, including relaxation or possibly a chemical reaction, all of which can be probed by monitoring time evolving vibrational transitions. Alternatively, vibrational excitation could precede an electronic probe—either a single UV, visible, or near-IR pulse or a full 2D pulse sequence—to monitor the influence of depositing energy directly into specific motional degrees of freedom. Processes such as charge or energy transfer can be significantly altered by non-equilibrium vibrational pumping.[56] Being able to access very different electronic transitions has long been used to study photoinduced processes in molecules and semiconductors, but so far, there has been little progress in marrying these measurements with multidimensional approaches.

Dual amplifiers (access to 12 orders of magnitude in time)

By employing a dual-amplifier system seeded by using a common titanium sapphire oscillator, the MMDS bridges time scales from the fastest femtosecond fluctuations to the much slower, potentially diffusive, micro- and millisecond regimes. This flexibility enables the triggering of nonequilibrium processes, which can then be followed with a choice of multidimensional probe. Since the timing between the lasers is controlled electronically, it is possible to access the full range from femtoseconds to milliseconds and beyond. The use of

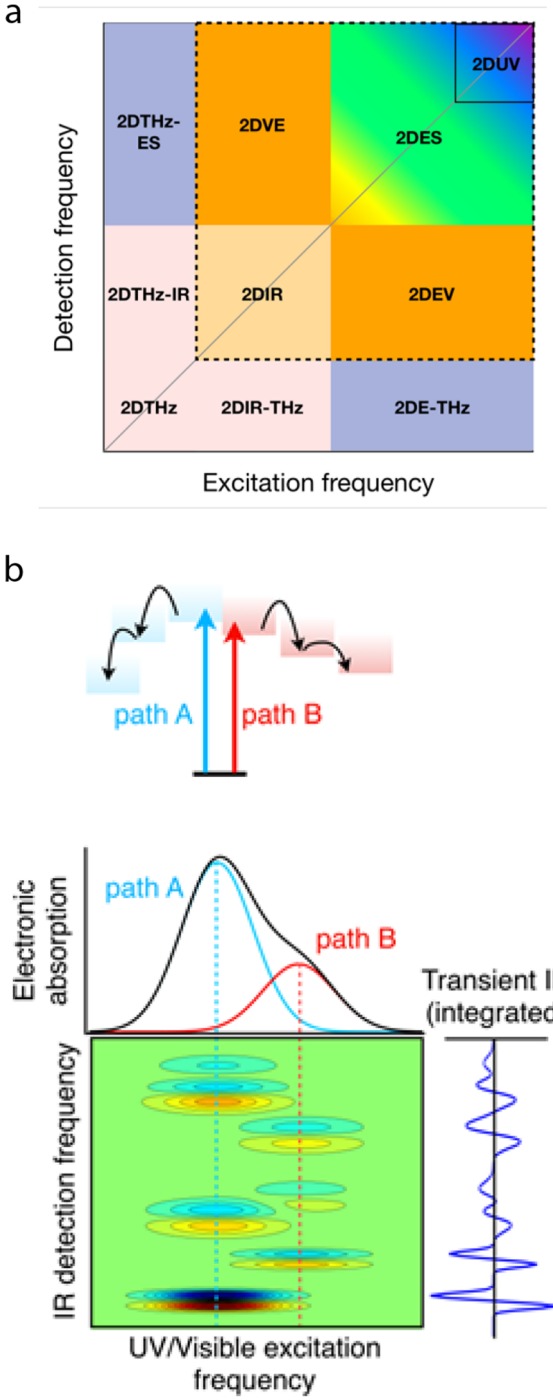

FIG. 3. (a) Illustration of existing and conceivable multispectral multidimensional spectroscopies spanning the THz-UV. The dashed box indicates capabilities of the MMDS. (b) Cartoon depicting the benefits of employing multispectral multidimensional spectroscopy for studying a system with overlapping electronic transitions that induce distinct photochemical or photophysical processes. As shown in (b), the correlation between excited electronic and detected vibrational transitions enables clear isolation of the distinct species which is difficult or impossible with transient 1D spectroscopy.

two kHz amplifiers (Spitfire Ace and Solstice, Spectra Physics), both seeded by using the same oscillator (MaiTai, Spectra Physics), enables simultaneous and independent access to the full UV-to-IR spectral range, as described below and depicted in Fig. 4. The dual-amplifier approach is mandatory to access long, micro-, and millisecond time delays required to fully sample hierarchical condensed phase dynamics ranging from protein folding to charge carrier migration in natural and artificial systems. The time delay between the amplifiers can be adjusted in steps of the 80 MHz oscillator's 12.5 ns round-trip time by digitally delaying the signal (Stanford Research System, DG535) sent to each amplifier's electro-optic device (a Pockels cell) with no moving parts. Delays shorter than 12.5 ns are achieved by using a standard multiply passed translation stage (Newport, IMS600LM). We note that similar dual amplifier setups are available at the Rutherford Appleton Lab (in which one amplifier is a narrowband ps system and the other is a short-pulse fs amplifier)[57–61] and in the lab of Prof. Peter Hamm (University of Zürich).[62]

Light sources of the MMDS (ultraviolet—Mid IR)

The spectral ranges of the different light sources of the MMDS are shown in Fig. 4, featuring both commercially available and home-built sources. The output of the 35-fs Spitfire amplifier pumps a commercial nonlinear optical parametric amplifier (NOPA) (TOPAS White, Light Conversion) using 700 μJ, while an additional 700 μJ is used to pump a home-built NOPA for broader bandwidth. The TOPAS White output can be tuned from 500 to 1000 nm with a typical pulse energy of 5–50 μJ. These high energy pulses are frequency doubled in an additional module inside the TOPAS White to produce narrow-band high energy UV pulses which are tunable from 250 to 375 nm and 420 to 500 nm. The home-built NOPA can be tuned from 490 to 750 nm with a typical pulse energy of 5-10 μJ.[63] A visible white light continuum is generated by focusing ~0.8 μJ of the 800 nm pulses either into a 5 mm thick sapphire window (450–780 nm) or into a 5 mm thick

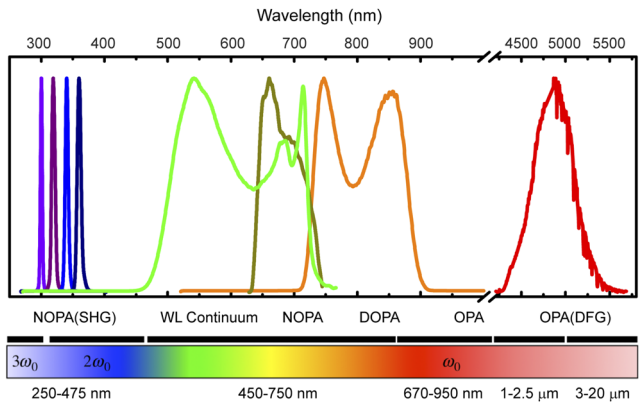

FIG. 4. Sources and overall spectral range available for multispectral multidimensional spectroscopy with the MMDS. The UV, WL continuum, and NOPA are generated using the Spitfire Ace, while the DOPA and mid-IR spectrum are generated using the Solstice Ace amplifier.

CaF_2 window (320–780 nm) that is continuously translated in order to avoid thermal damage. The near-IR wavelengths of the continuum spanning 820–1100 nm can also be used for probing. Frequency doubled 800 nm pulses are focused on the CaF_2 window to generate UV white light continuum spanning 260–370 nm. The 100-fs Solstice amplifier is used to pump a commercial near-IR OPA (TOPAS Twins, Light Conversion) that has two independently tunable outputs. The signal (1160–1550 nm) and idler (1550-2600 nm) from one of the outputs are used to generate mid-IR pulses by difference frequency generation. The signal from the output of the other port is used to generate a white light continuum spanning the near-IR (600–970 nm). This pulse acts as seed in a home-built degenerate optical parametric amplifier (DOPA) pumped by the second harmonic of the 100 fs fundamental from the Solstice.[64] The amplified broadband pulses span 670–950 nm with a typical output energy of 8 μJ.

2DES and 2DIR spectroscopy

2D Fourier transform spectroscopy in the visible and mid-IR regions is a well developed and mature technique and can readily be implemented with pulse-shapers. In the visible, the MMDS employs an acousto-optic pulse-shaper (Dazzler, Fastlite), a small optical element the size of a deck of cards that can be inserted into the beam to produce a programmable pulse train, where each laser shot (1 kHz repetition rate) can be programmed differently. The Ogilvie lab has previously demonstrated the use of the Dazzler for 2DES.[23,25,29] For 2DIR experiments, the MMDS employs an acousto-optic pulse-shaper (PhaseTech) developed by the Zanni lab.[22,26,64,65]

2DUV spectroscopy

Progress in developing 2DUV spectroscopy has been slow relative to the IR and visible regimes.[66] Fortunately there have been some recent developments that will speed its implementation and broaden its applications.[67–71] Challenges include broadband UV pulse generation, dispersion compensation, and the control over the coherence time (t_1, the delay between the first two excitation pulses). Pulse generation and the maintenance of short pulses are both linked to the same fundamental fact that since all materials eventually absorb in the UV, being close to resonance necessarily increases material dispersion. Finally, given the short wavelengths of UV light, the requirements for any interferometer to maintain stability are extremely difficult to meet, given that path length fluctuations on the order of $\lambda/100$ can limit the useful interference needed for Fourier transform spectroscopy. To date, there have been several approaches to implementing 2DUV spectroscopy. Weinacht *et al.* used a transverse acousto-optic pulse shaper to create the phase-controlled excitation pulse pair.[70,71] Moran *et al.* and Brixner *et al.* leveraged passive phase stability of a diffractive optic approach, commonly used in 2DES.[66,72,73] Brixner *et al.* also adopted an all-reflective common-path approach in the visible.[74] Prokhorenko *et al.* demonstrated the broadest bandwidth Fourier-transform 2DUV to date, using an all-reflective diffractive-optic approach and a frequency-doubled NOPA to provide spectra spanning ~250-300 nm.[75,76] Chergui *et al.* employed the hybrid time-frequency domain strategy which has found wide adoption in the infrared.[77] The hybrid method does not require the bandwidth to be contained simultaneously in a single pulse, but instead a narrower band pump is tuned (or filtered) across the absorption spectrum. Since UV transitions are typically very broad, even a "narrowband" UV pulse can have a Fourier transform time duration of <100 fs, providing high enough time resolution for many applications.

The MMDS employs a UV Dazzler pulse-shaper, in principle enabling both Fourier transform and hybrid frequency-time approaches; the latter places relaxed requirements on the degree of pulse compression needed since the pulse shaper is capable of fully compensating dispersion over a narrow spectral range. Krebs *et al.*[78] demonstrated the use of UV Dazzler to perform 2D UV measurements in the pump-probe geometry. Our current UV sources are not sufficiently broadband to motivate use of the Fourier transform approach. An alternative approach of generating broadband phase modulated UV pulse pairs is through sum frequency mixing of compressed broadband visible pulse pairs with a sufficiently long 800 nm pulse in a type II BBO as demonstrated recently by Cerullo *et al.*[79] The current 2DUV capabilities of the MMDS feature high energy tunable narrow-band (2-3 nm FWHM) UV pump pulses spanning 250–380 nm and 420–460 nm and a UV white light continuum probe generated by focusing 400 nm pulses on a CaF_2 window to be discussed in further detail below.

MULTISPECTRAL MULTIDIMENSIONAL SPECTROSCOPY

Two-color 2DES and 2DIR are now well established methods.[25,80,81] A unique capability of the MMDS is the generation of mixed spectral sequences, combining UV, visible, and IR excitation and probing. In the pump-probe geometry, the requirements of phase-matching are significantly reduced, enabling the mixing of vastly different frequencies. In addition, the probe is detected directly by using the CCD, making broadband continuum practical probe light sources due to their lower power.[23] By combining the various light sources discussed above in the pump-probe geometry, the MMDS is capable of a wide variety of multispectral measurements. Below we illustrate this capability with several spectroscopies combining sources in the UV, visible, and mid-IR.

2DES with a continuum probe

2DES with a continuum probe is achieved by employing pulses from the home-built NOPA or DOPA as the pump source depending on the sample of interest and the white light continuum pulses in the visible as the probe pulse. As described earlier, we perform the experiments in the pump-probe geometry in an all-reflective spectrometer. Broadband probing using white light supercontinuum generated in bulk crystals has proven to be a versatile tool in the ultrafast community and has been implemented more recently in multidimensional spectroscopic experiments in combination with broadband visible,[28,82,83] UV,[78] and supercontinuum

pump pulses.[84] These pulses are linearly chirped owing to the large frequency content. This necessitates post-process correction in order to retrieve the temporally aligned (along detection axis) 2D spectrum, as was illustrated by Tekavec *et al.*[55] The phase stable pairs of pump pulses are generated and partially compressed using the Dazzler. The pump and probe pulses are focused to $1/e^2$ spots of 250 μm and 170 μm, respectively. The relative delay between the pump and probe pulse is controlled via a retroreflector mounted on a computer controlled delay stage. The spectrally resolved intensity of each laser shot is measured at the full 1 kHz repetition rate with an Horiba Jobin Yvon (iHR320) spectrometer and a CCD camera (Pixis, Princeton Instruments). Given that we adopted the pump-probe geometry, the signal is emitted in the probe direction with the probe acting as both the third excitation pulse and the local oscillator field for heterodyne detection. Background free absorptive 2DES spectra were constructed by subtracting the phase-cycled data ($S(\Delta\phi = 0) - S(\Delta\phi = \pi)$) and Fourier transforming along the τ axis to generate the excitation axis.[25]

We illustrate the usefulness of 2DES using a continuum probe by showing representative data (Fig. 5) on the WM250V mutant of the bacterial reaction center (BRC) from *R. capsulatus*.[54] The BRC is a macromolecule composed of six chromophores (4 bacteriochlorophyll a and 2 bacteriopheophytin) arranged in two almost identical branches. It has three well defined absorption peaks in the near-IR region (Q_y) and slightly weaker peaks in the visible (Q_x) as a result of excitonic coupling between the chromophores. Upon photoexcitation, there is rapid energy transfer within the chromophores ultimately leading to charge separation within several picoseconds. Here we show the real absorptive 2D spectrum acquired at T = 1.5 ps upon exciting the Q_y transitions using the broadband pulses generated from the DOPA and detecting the Q_x transitions using the white light continuum from sapphire in the visible. A strong negative signal due to the excited-state absorption (ESA) of the excited Q_y molecules is detected in the Q_x region for all the excitation frequencies. The ground-state bleaching (GSB) of the Q_x transitions are detected as positive signals on top of the broad ESA signal. The signal between 16 200 cm^{-1} and 17 000 cm^{-1} is due to the GSB of the Q_x transitions of the bacteriochlorophyll molecules, while 18 200 cm^{-1} and 18 400 cm^{-1} is due to the GSB of the Qx transitions of the bacteriopheophytin molecules.

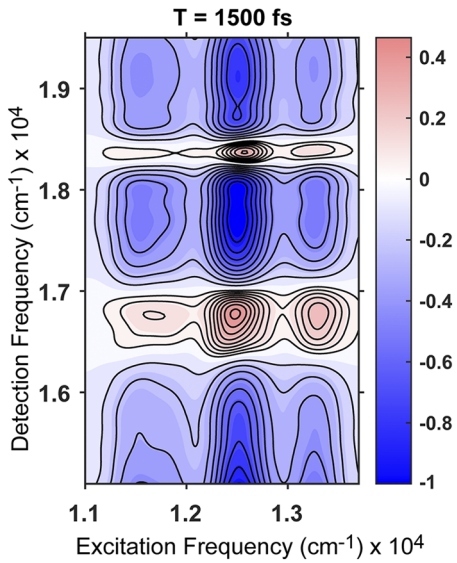

FIG. 5. Real absorptive 2D map at waiting time, T = 1.5 ps, obtained by exciting the Q_y transitions of the WM250V mutant of BRC and detecting the photoinduced changes in the Q_x transitions.[54] Contours are plotted in steps of 5% starting at 10%.

2DUV with a continuum probe

2DUV is currently implemented by scanning the narrow UV pump spectrum across the absorption spectrum of the sample of interest while probing with a broadband UV or visible continuum in a pump-probe geometry. The use of narrow pump pulses limits the time resolution of the experiments to ~250 fs. A vast majority of biomolecules have broad absorption in the UV, and disentangling the contributions of overlapping transitions from the constituent amino acids will help us better understand the mechanisms of charge generation, photo-protection, etc. To demonstrate the UV capability of MMDS, we studied the excitation wavelength dependence of the ground and excited state dynamics of reduced Flavin Mononucleotide ($FMNH^-$). Flavins are an important class of photoactive cofactors that are involved in photorepair of UV-damaged DNA as well as in the photosensory apparatus of birds.[85] Though Flavins in different oxidation states play different roles, the reduced form is known to play the most important roles. The nature of transitions giving rise to the absorption spectra of reduced Flavins has been the subject of debate for some time. According to a recent study reporting the results of Stark spectroscopy of reduced Flavins, the red part of the absorption spectrum between 340 and 500 nm is composed of nearly parallel overlapping electronic transitions as opposed to earlier reports of a single electronic transition.[86] The $FMNH^-$ sample was prepared following the methods of Brazard *et al.*[87] A 2D plot constructed using the transient absorption signal corresponding to each excitation wavelength at T = 1 ps is shown in Fig. 6. The excitation wavelength region between 370 and 420 nm is not covered by the NOPA due to the significant instability of the white light continuum. The truncated steady state spectrum of $FMNH^-$ is plotted along the excitation axis. The pulse energy of the different UV pulses was kept constant using a variable ND filter, and the excitation probability was kept around 5%. The transient signal consists of either a broad ESA or two ESA bands and a stimulated emission band at 440 nm. The maximum signal is concentrated between 350 and 360 nm and has a slight structure along the excitation axis. For the 420–460 nm excitation region, the signal is omitted between 440 and 480 nm due to contamination from pump scatter. Global analysis of the data promises to provide insight into the electronic structure and excited state relaxation processes in this system.

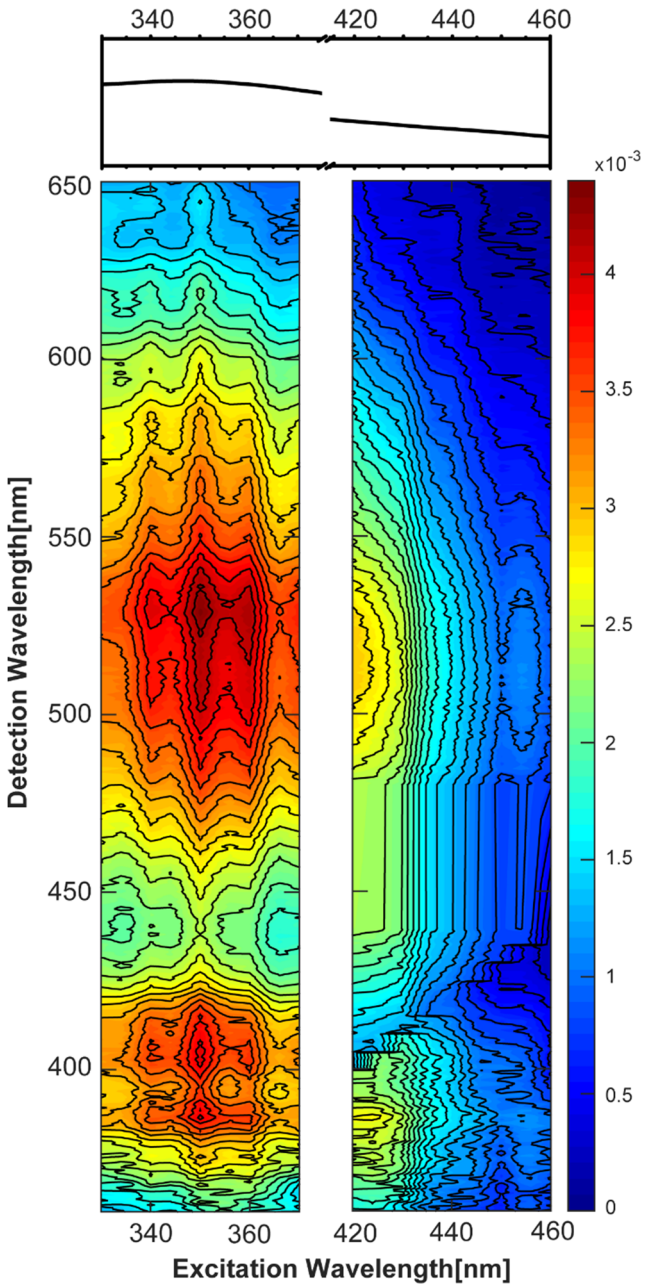

FIG. 6. 2D UV pump/visible probe spectra of reduced Flavin mononucleotide recorded at a delay time of T = 1 ps. The narrow UV pump is scanned from 330 to 370 nm and from 420 to 460 nm in steps of 5 nm. The steady state absorption spectrum of the sample (black) is plotted on the top. The spectrum has been truncated between 370 and 420 nm in order to match the range of the 2D plots.

2D electronic vibrational spectroscopy (2DEV)

The combination of infrared and visible or UV pulses enables a direct mapping between, in the case of molecular systems, vibrational and electronic degrees of freedom. Both typically exhibit inhomogeneous broadening and spectral overlap of distinct transitions. By correlating excited electronic frequencies with detected IR frequencies, we will be able to use the chemical specificity of vibrational bands to help assign the structural nature of electronic transitions even in the presence of environmentally induced spectral heterogeneity. Using the dynamical aspects of 2D spectroscopy by varying the waiting time, we will be able to follow excited electronic state dynamics by viewing the transient influence over well-defined vibrational probes. By pumping with IR pulses, we will be able to assess the state-specificity of excited state energy and charge transfer given, for example, excitation of a bridging vibration.[56,88]

2DEV was demonstrated first with excitation in the visible range (500–800 nm) by the Fleming group[49] and later in the UV range (390–410 nm) by the Khalil group.[52] Recently, 2DEV has been applied to study the photoexcited dynamics in a few molecular systems, such as laser dyes,[49] light-harvesting complex II,[47] a model carotenoid complex,[48] chlorophylls,[46] and metal complexes.[52] Here we demonstrate the 2DEV capability of the MMDS by studying the photosensitized dye—di-tetrabutylammonium *cis*-bis(isothiocyanato)bis(2,2′-bipyridyl-4,4′-dicarboxylato)ruthenium(II) (N719).

Our 2DEV setup adopts our previous design of the pulse-shaper-based pump-probe geometry 2DES.[25] An acousto-optic programmable dispersive filter (AOPDF) is used to precisely control the time delay between two pump pulses. A homebuilt visible NOPA[63] (490–750 nm) and a near-IR DOPA[41] (670–950 nm) are used as the pump light sources in our setup, and these two pumps are switchable via inserting/removing several mirrors on magnetic mounts. The pump beam is focused at the sample position by a 40 cm lens, and the diameter ($1/e^2$) is ~250 μm. The probe pulse is generated via a home-built difference frequency generation (DFG) which is described in the section on light sources. The probe beam is focused by using a 10 cm parabolic mirror, and the diameter ($1/e^2$) at focus is ~200 μm. The pump and probe are spatially overlapped at the sample position. The signal is heterodyne detected with the transmitted probe beam using a Horiba Jobin Yvon spectrometer (iHR320) and a 64-pixel HgCdTe (MCT) array detector (Infrared Systems Development, FPAS-6414). The detected signal includes both linear response and third-order response such as pump-probe and 2DEV signals. The desired 2DEV signal is extracted from the background via Fourier transformation and phase cycling. Although these two spectra in 2DEV have the same pulse sequence as 2DES or 2DIR, the emitted electric field in the rephasing spectrum does not recover the phase of electronic coherence at the time $t = \tau$. Thus rephasing of 2DEV does not provide a straightforward way to disentangle the inhomogeneous and homogeneous broadening.

To study the dye N719, a 12 fs, 40 nJ NOPA beam centered at ~540 nm is used to excite the sample. The probe, generated by DFG, is centered at ~4.800 μm with a FWHM >300 nm. The probe pulse energy is kept below 100 nJ before the sample to avoid both nonlinear processes induced by the probe and saturation of the detector. The instrument response is estimated to be ~100 fs based on pump-probe measurements of a piece

of silica wafer. For each 2D spectrum, t_1 is scanned from –40 to 0 fs with a step size of 0.4 fs. The data were averaged over 400 shots for each coherence time (t_1 or t). The N719 solution is stored in a 380 μm customized CaF_2 cuvette during the measurement at room temperature.

Figure 7 displays a representative absorptive 2DEV spectrum of N719 in N,N-dimethylformamide (DMF). The 2DEV spectrum exhibits one positive peak at 2112 cm^{-1} and two distinctive negative peaks at 2080 cm^{-1} and 2033 cm^{-1}. All three peaks originate from CN stretching modes. The first peak stems from the ground electronic state and the latter two are assigned to the anti-symmetric and symmetric modes, respectively, in the excited electronic state. Similar features have been observed in other dye molecules by 2DIR[89] and visible-pump mid-IR probe pump-probe experiments.[90] This observation exemplifies the utility of the MMDS in revealing the tuning of vibrational molecular levels following electronic excitation.

While here we have demonstrated 2DEV, the MMDS will also be capable of performing 2DVE as previously demonstrated by the Khalil group.[50,51,53] To enable 2DVE measurements, the pump-probe geometry will be used, in which the mid-IR pulse-shaper creates the collinear pump pulse pair, and the optical probe pulse will originate from the NOPA or DOPA. The interference between the signal and the probe will be directed to the CCD camera of the pump-probe geometry 2DES setup for detection.

2D spectroscopy beyond nanosecond time scales

Taking advantage of dual amplifiers with a common seed, our setup is versatile to record dynamics from ns to ms. Figure 8 shows an absorption spectrum and a representative 2DEV absorptive spectrum of an organic donor-acceptor blend at 40 ns. This blend is composed of a conjugated polymer, poly[(2,6-(4,8-bis(5-(2-ethylhexyl)thiophen-2-yl)-benzo[1,2-b:4,5-b']dithiophene))-alt-(5,5-(1′,3′-di-2-thienyl-5′,7′-bis(2-ethylhexyl)benzo[1′,2′-c:4′,5′-c′]dithiophene-4,8-dione)] (PBDB-T), and a small molecule acceptor, 3,9-bis(2-methylene-(3-(1,1-dicyanomethylene)-indanone))-5,5,11,11-tetrakis(4-hexylphenyl)-dithieno[2,3-d:2′,3′-d′]-s-indaceno [1,2-b:5,6-b′]dithiophene (ITIC). 2DEV exhibits a broadband

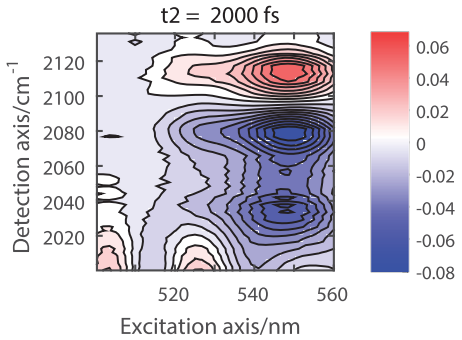

FIG. 7. Absorptive 2DEV of N719 in DMF at a waiting time of T = 2 ps. Contours are drawn at levels of 10%.

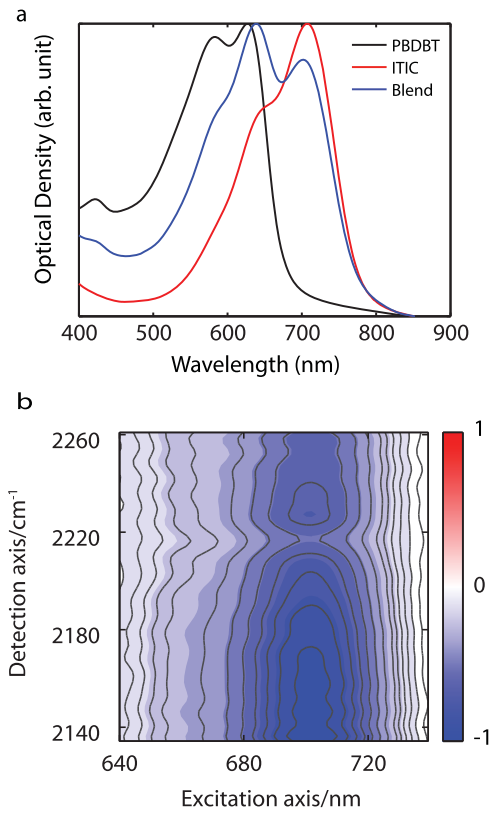

FIG. 8. (a) Absorption of the PBDBT, ITIC, and PBDBT/ITIC blend; (b) 2DEV absorptive spectra of the PBDBT/ITIC blend at T = 40 ns; contour intervals are 5% from 0% to 0.2% and 10% from 0.2 to 1.

photoinduced absorption which can be attributed to the polarons according to previous studies.[91,92] On top of the photoinduced absorption, a positive-going peak at around 2222 cm^{-1} is also observed. This peak stems from the GSB of the CN stretching mode in the acceptor. It has been demonstrated that such a vibrational mode can be used as a spectator to monitor the carrier migration dynamics in the organic photovoltaic materials.[93]

CONCLUSIONS

We have demonstrated a dual-amplifier-based MMDS that enables pulse-shaper-based one color 2D spectroscopy in the UV, visible, and IR regimes as well as mixed frequency spectroscopies, of which we have demonstrated 2DEV and 2DES/2DUV with a continuum probe. The flexible setup and broad range of sources of the MMDS can also be used in a wide range of other multispectral multidimensional spectroscopies, such as transient 2D spectroscopy wherein an actinic pump initiates a process of interest, and a 2D pulse sequence is then used as a probe over time scales spanning fs seconds. Other surface-specific probes, such as second harmonic or sum-frequency generation, could also be readily implemented and combined with 2D excitation. In addition,

"pump-push-probe" methods could be used. For example, studies of photovoltaics could employ an IR "push" pulse inserted before the probe pulse in a 2DES experiment to understand the effect of IR excitation of particular vibrational modes on charge transfer processes.[94–97] Considering these capabilities, the MMDS provides the opportunity to perform a wide variety of experiments on atomic, molecular, and material systems spanning broad spectral and temporal regimes.

ACKNOWLEDGMENTS

The authors gratefully acknowledge the support of the National Science Foundation through instrumentation Grant No. CHE-1428479. Y. Song and J. P. Ogilvie acknowledge support from the Office of Basic Energy Sciences, the US Department of Energy under Grant No. DE-FG02-07ER15904 for the development of the 2DEV capability. Y. Song acknowledges the support of the Natural Sciences and Engineering Council of Canada (NSERC) for a Postdoctoral Fellowship. V. Policht acknowledges support from the National Science Foundation through Grant No. PHY-0748470, and R. Sechrist acknowledges funding from the National Science Foundation Graduate Fellowship program. R. Duan, V. P. Roy, and K. J. Kubarych acknowledge support from the National Science Foundation through Grant No. CHE-1565795.

REFERENCES

[1]Y. Tanimura and S. Mukamel, "2-dimensional femtosecond vibrational spectroscopy of liquids," J. Chem. Phys. **99**, 9496–9511 (1993).
[2]M. Cho, "Coherent two-dimensional optical spectroscopy," Chem. Rev. **108**, 1331–1418 (2008).
[3]W. Zhuang, T. Hayashi, and S. Mukamel, "Coherent multidimensional vibrational spectroscopy of biomolecules: Concepts, simulations, and challenges," Angew. Chem., Int. Ed. **48**, 3750–3781 (2009).
[4]J. P. Ogilvie and K. J. Kubarych, "Multidimensional electronic and vibrational spectroscopy: An ultrafast probe of molecular relaxation and reaction dynamics," Adv. At., Mol., Opt. Phys. **57**, 249–321 (2009).
[5]M. Khalil, N. Demirdoven, and A. Tokmakoff, "Coherent 2D IR spectroscopy: Molecular structure and dynamics in solution," J. Phys. Chem. A **107**, 5258–5279 (2003).
[6]D. Jonas, "Two-dimensional femtosecond spectroscopy," Annu. Rev. Phys. Chem. **54**, 425–463 (2003).
[7]J. Zheng, K. Kwak, and M. Fayer, "Ultrafast 2D IR vibrational echo spectroscopy," Acc. Chem. Res. **40**, 75–83 (2007).
[8]T. Elsaesser, "Two-dimensional infrared spectroscopy of intermolecular hydrogen bonds in the condensed phase," Acc. Chem. Res. **42**, 1220–1228 (2009).
[9]P. Hamm and M. T. Zanni, *Concepts and Methods of 2D Infrared Spectroscopy* (Cambridge University Press, 2011).
[10]Y. Kim and R. Hochstrasser, "Applications of 2D IR spectroscopy to peptides, proteins, and hydrogen-bond dynamics," J. Phys. Chem. B **113**, 8231–8251 (2009).
[11]J. D. Zimmerman *et al.*, "Use of additives in porphyrin-tape/C-60 near-infrared photodetectors," Org. Electron. **12**, 869–873 (2011).
[12]M. J. Nee, C. R. Baiz, J. M. Anna, R. McCanne, and K. J. Kubarych, "Multilevel vibrational coherence transfer and wavepacket dynamics probed with multidimensional IR spectroscopy," J. Chem. Phys. **129**, 084503 (2008).
[13]C. R. Baiz, P. L. McRobbie, N. K. Preketes, K. J. Kubarych, and E. Geva, "Two-dimensional infrared spectroscopy of dimanganese decacarbonyl and its photoproducts: An *ab initio* study," J. Phys. Chem. A **113**, 9617–9623 (2009).
[14]C. R. Baiz, P. L. Mcrobbie, J. M. Anna, E. Geva, and K. J. Kubarych, "Two dimensional infrared spectroscopy of metal carbonyls," Acc. Chem. Res. **42**, 1395–1404 (2009).
[15]J. T. King, J. M. Anna, and K. J. Kubarych, "Solvent-hindered intramolecular vibrational redistribution," Phys. Chem. Chem. Phys. **13**, 5579–5583 (2011).
[16]C. R. Baiz, K. J. Kubarych, E. Geva, and E. L. Sibert, "Local-mode approach to modeling multidimensional infrared spectra of metal carbonyls," J. Phys. Chem. A **115**, 5354–5363 (2011).
[17]C. R. Baiz, K. J. Kubarych, and E. Geva, "Molecular theory and simulation of coherence transfer in metal carbonyls and its signature on multidimensional infrared spectra," J. Phys. Chem. B **115**, 5322–5339 (2011).
[18]L. M. Kiefer, J. T. King, and K. J. Kubarych, "Dynamics of rhenium photocatalysts revealed through ultrafast multidimensional spectroscopy," Acc. Chem. Res. **48**, 1123–1130 (2015).
[19]L. M. Kiefer and K. J. Kubarych, "Two-dimensional infrared spectroscopy of coordination complexes: From solvent dynamics to photocatalysis," Coord. Chem. Rev. **372**, 153–178 (2018).
[20]L. DeFlores, R. Nicodemus, and A. Tokmakoff, "Two dimensional Fourier transform spectroscopy in the pump-probe geometry," Opt. Lett. **32**, 2966–2968 (2007).
[21]D. Strasfeld, S. Shim, and M. Zanni, "New advances in mid-IR pulse shaping and its application to 2D IR spectroscopy and ground-state coherent control," Adv. Chem. Phys. **141**, 1–28 (2009).
[22]E. Grumstrup, S. Shim, M. Montgomery, N. Damrauer, and M. Zanni, "Facile collection of two-dimensional electronic spectra using femtosecond pulse-shaping technology," Opt. Express **15**, 16681–16689 (2007).
[23]P. F. Tekavec, J. A. Myers, K. L. M. Lewis, and J. P. Ogilvie, "Two dimensional electronic spectroscopy with a continuum probe," Opt. Lett. **34**, 1390–1392 (2009).
[24]S. Faeder and D. Jonas, "Two-dimensional electronic correlation and relaxation spectra: Theory and model calculations," J. Phys. Chem. A **103**, 10489–10505 (1999).
[25]J. A. Myers, K. L. M. Lewis, P. F. Tekavec, and J. P. Ogilvie, "Two-color two-dimensional Fourier transform electronic spectroscopy with a pulse-shaper," Opt. Express **16**, 17420–17428 (2008).
[26]S. H. Shim, D. B. Strasfeld, Y. L. Ling, and M. T. Zanni, "Automated 2D IR spectroscopy using a mid-IR pulse shaper and application of this technology to the human islet amyloid polypeptide," Proc. Natl. Acad. Sci. U. S. A. **104**, 14197–14202 (2007).
[27]J. E. Laaser, W. Xiong, and M. T. Zanni, "Time-domain SFG spectroscopy using mid-IR pulse shaping: Practical and intrinsic advantages," J. Phys. Chem. B **115**, 2536–2546 (2011).
[28]S. K. K. Kumar, A. Tamimi, and M. D. Fayer, "Comparisons of 2D IR measured spectral diffusion in rotating frames using pulse shaping and in the stationary frame using the standard method," J. Chem. Phys. **137**, 184201 (2012).
[29]P. F. Tekavec, J. A. Myers, K. L. M. Lewis, F. D. Fuller, and J. P. Ogilvie, "Effects of chirp on two-dimensional Fourier transform electronic spectra," Opt. Express **18**, 11015–11024 (2010).
[30]K. L. M. Lewis and J. P. Ogilvie, "Probing photosynthetic energy and charge transfer with two-dimensional electronic spectroscopy," J. Phys. Chem. Lett. **3**, 503–510 (2012).
[31]S. H. Shim and M. T. Zanni, "How to turn your pump-probe instrument into a multidimensional spectrometer: 2D IR and vis spectroscopies via pulse shaping," Phys. Chem. Chem. Phys. **11**, 748–761 (2009).
[32]C. T. Middleton, A. M. Woys, S. S. Mukherjee, and M. T. Zanni, "Residue specific structural kinetics of proteins through the union of isotope labeling, mid-IR pulse shaping, and coherent 2D IR spectroscopy," Methods **52**, 12–22 (2010).
[33]M. Khalil, N. Demirdoven, and A. Tokmakoff, "Obtaining absorptive line shapes in two-dimensional infrared vibrational correlation spectra," Phys. Rev. Lett. **90**, 047401 (2003).

[34]J. Savolainen, S. Ahmed, and P. Hamm, "Two-dimensional Raman-terahertz spectroscopy of water," Proc. Natl. Acad. Sci. U. S. A. **110**, 20402–20407 (2013).
[35]C. Somma, K. Reimann, C. Flytzanis, T. Elsaesser, and M. Woerner, "High field terahertz bulk photovoltaic effect in lithium niobate," Phys. Rev. Lett. **112**, 146602 (2014).
[36]I. A. Finneran, R. Welsch, M. A. Allodi, T. F. Miller III, and G. A. Blake, "Coherent two-dimensional terahertz-terahertz-Raman spectroscopy," Proc. Natl. Acad. Sci. U. S. A. **113**, 6857–6861 (2016).
[37]J. Lu *et al.*, "Nonlinear two-dimensional terahertz photon echo and rotational spectroscopy in the gas phase," Proc. Natl. Acad. Sci. U. S. A. **113**, 11800–11805 (2016).
[38]C. W. Berry, N. Wang, M. R. Hashemi, M. Unlu, and M. Jarrahi, "Significant performance enhancement in photoconductive terahertz optoelectronics by incorporating plasmonic contact electrodes," Nat. Commun. **4**, 1622 (2013).
[39]H. Michel, "The mechanism of proton pumping by cytochrome c oxidase," Proc. Natl. Acad. Sci. U. S. A. **95**, 12819–12824 (1998).
[40]J. Liu, K. Okamura, Y. Kida, T. Teramoto, and T. Kobayashi, "Clean sub-8-fs pulses at 400 nm generated by a hollow fiber compressor for ultraviolet ultrafast pump-probe spectroscopy," Opt. Express **18**, 20645–20650 (2010).
[41]A. M. Siddiqui, G. Cirmi, D. Brida, F. X. Kartner, and G. Cerullo, "Generation of <7 fs pulses at 800 nm from a blue-pumped optical parametric amplifier at degeneracy," Opt. Lett. **34**, 3592–3594 (2009).
[42]A. Jasaitis, F. Rappaport, E. Pilet, U. Liebl, and M. H. Vos, "Activationless electron transfer through the hydrophobic core of cytochrome c oxidase," Proc. Natl. Acad. Sci. U. S. A. **102**, 10882–10886 (2005).
[43]C. Ventalon, J. M. Fraser, M. H. Vos, A. Alexandrou, J. L. Martin, and M. Joffre, "Coherent vibrational climbing in carboxyhemoglobin," Proc. Natl. Acad. Sci. U. S. A. **101**, 13216–13220 (2004).
[44]B. L. McClain, I. J. Finkelstein, and M. D. Fayer, "Dynamics of hemoglobin in human erythrocytes and in solution: Influence of viscosity studied by ultrafast vibrational echo experiments," J. Am. Chem. Soc. **126**, 15702–15710 (2004).
[45]S. Bagchi, B. T. Nebgen, R. F. Loring, and M. D. Fayer, "Dynamics of a myoglobin mutant enzyme: 2D IR vibrational echo experiments and simulations," J. Am. Chem. Soc. **132**, 18367–18376 (2010).
[46]N. H. C. Lewis and G. R. Fleming, "Two-dimensional electronic-vibrational spectroscopy of chlorophyll a and b," J. Phys. Chem. Lett. **7**, 831–837 (2016).
[47]N. H. C. Lewis *et al.*, "Observation of electronic excitation transfer through light harvesting complex II using two-dimensional electronic-vibrational spectroscopy," J. Phys. Chem. Lett. **7**, 4197–4206 (2016).
[48]T. A. A. Oliver and G. R. Fleming, "Following coupled electronic-nuclear motion through conical intersections in the ultrafast relaxation of beta-apo-8′-carotenal," J. Phys. Chem. B **119**, 11428–11441 (2015).
[49]T. A. A. Oliver, N. H. C. Lewis, and G. R. Fleming, "Correlating the motion of electrons and nuclei with two-dimensional electronic-vibrational spectroscopy," Proc. Natl. Acad. Sci. U. S. A. **111**, 16628 (2014); "Correlating the motion of electrons and nuclei with two-dimensional electronic-vibrational spectroscopy," **111**, 10061 (2014).
[50]T. L. Courtney, Z. W. Fox, L. Estergreen, and M. Khalil, "Measuring coherently coupled intramolecular vibrational and charge-transfer dynamics with two-dimensional vibrational electronic spectroscopy," J. Phys. Chem. Lett. **6**, 1286–1292 (2015).
[51]T. L. Courtney, Z. W. Fox, K. M. Slenkamp, and M. Khalil, "Two dimensional vibrational-electronic spectroscopy," J. Chem. Phys. **143**, 154201 (2015).
[52]J. D. Gaynor, T. L. Courtney, M. Balasubramanian, and M. Khalil, "Fourier transform two-dimensional electronic-vibrational spectroscopy using an octave-spanning mid-IR probe," Opt. Lett. **41**, 2895–2898 (2016).
[53]J. D. Gaynor and M. Khalil, "Signatures of vibronic coupling in two-dimensional electronic-vibrational and vibrational-electronic spectroscopies," J. Chem. Phys. **147**, 094202 (2017).
[54]A. Konar *et al.*, "Electronic interactions in the bacterial reaction center revealed by two-color 2D electronic spectroscopy," J. Phys. Chem. Lett. **9**, 5219 (2018).
[55]P. A. Tekavec, K. L. Lewis, F. D. Fuller, J. A. Myers, and J. P. Ogilvie, "Toward broad bandwidth 2-D electronic spectroscopy: Correction of chirp from a continuum probe," IEEE J. Sel. Top. Quantum Electron. **18**, 210 (2011).
[56]Z. W. Lin *et al.*, "Modulating unimolecular charge transfer by exciting bridge vibrations," J. Am. Chem. Soc. **131**, 18060 (2009).
[57]C. Bellota-Anton *et al.*, "Spectroscopic analysis of protein Fe-NO complexes," Biochem. Soc. Trans. **39**, 1293–1298 (2011).
[58]A. I. Stewart *et al.*, "Determination of the photolysis products of FeFe hydrogenase enzyme model systems using ultrafast multidimensional infrared spectroscopy," Inorg. Chem. **49**, 9563–9573 (2010).
[59]S. Kaziannis *et al.*, "Femtosecond to microsecond photochemistry of a FeFe hydrogenase enzyme model compound," J. Phys. Chem. B **114**, 15370–15379 (2010).
[60]R. Kania *et al.*, "Investigating the vibrational dynamics of a 17e-metallocarbonyl intermediate using ultrafast two dimensional infrared spectroscopy," Phys. Chem. Chem. Phys. **12**, 1051–1063 (2010).
[61]A. I. Stewart *et al.*, "Structure and vibrational dynamics of model compounds of the [FeFe]-hydrogenase enzyme system via ultrafast two-dimensional infrared spectroscopy," J. Phys. Chem. B **112**, 10023–10032 (2008).
[62]J. Bredenbeck, J. Helbing, and P. Hamm, "Continuous scanning from picoseconds to microseconds in time resolved linear and nonlinear spectroscopy," Rev. Sci. Instrum. **75**, 4462–4466 (2004).
[63]T. Wilhelm, J. Piel, and E. Riedle, "Sub-20-fs pulses tunable across the visible from a blue-pumped single-pass noncollinear parametric converter," Opt. Lett. **22**, 1494–1496 (1997).
[64]S. Shim, D. Strasfeld, and M. Zanni, "Generation and characterization of phase and amplitude shaped femtosecond mid-IR pulses," Opt. Express **14**, 13120–13130 (2006).
[65]S. Shim, D. Strasfeld, E. Fulmer, and M. Zanni, "Femtosecond pulse shaping directly in the mid-IR using acousto-optic modulation," Opt. Lett. **31**, 838–840 (2006).
[66]B. A. West and A. M. Moran, "Two-dimensional electronic spectroscopy in the ultraviolet wavelength range," J. Phys. Chem. Lett. **3**, 2575–2581 (2012).
[67]C. A. Rivera, S. E. Bradforth, and G. Tempea, "Gires-Tournois interferometer type negative dispersion mirrors for deep ultraviolet pulse compression," Opt. Express **18**, 18615–18624 (2010).
[68]Y. Kida, J. Liu, T. Teramoto, and T. Kobayashi, "Sub-10 fs deep-ultraviolet pulses generated by chirped-pulse four-wave mixing," Opt. Lett. **35**, 1807–1809 (2010).
[69]B. A. West, P. G. Giokas, B. P. Molesky, A. D. Ross, and A. M. Moran, "Toward two-dimensional photon echo spectroscopy with 200 nm laser pulses," Opt. Express **21**, 2118–2125 (2013).
[70]C. H. Tseng, P. Sandor, M. Kotur, T. C. Weinacht, and S. Matsika, "Two dimensional Fourier transform spectroscopy of adenine and uracil using shaped ultrafast laser pulses in the deep UV," J. Phys. Chem. A **116**, 2654–2661 (2012).
[71]C. H. Tseng, S. Matsika, and T. C. Weinacht, "Two-dimensional ultrafast Fourier transform spectroscopy in the deep ultraviolet," Opt. Express **17**, 18788–18793 (2009).
[72]B. A. West, J. M. Womick, and A. M. Moran, "Probing ultrafast dynamics in adenine with mid-UV four-wave mixing spectroscopies," J. Phys. Chem. A **115**, 8630–8637 (2011).
[73]U. Selig *et al.*, "Coherent two-dimensional ultraviolet spectroscopy in fully noncollinear geometry," Opt. Lett. **35**, 4178–4180 (2010).
[74]U. Selig *et al.*, "Inherently phase-stable coherent two-dimensional spectroscopy using only conventional optics," Opt. Lett. **33**, 2851–2853 (2008).
[75]V. Prokhorenko, A. Picchiotti, S. Maneshi, and R. J. D. Miller, in *The 19th International Conference on Ultrafast Phenomena* (Springer, Okinawa, 2014).
[76]V. I. Prokhorenko, A. Picchiotti, M. Pola, A. G. Dijkstra, and R. J. D. Miller, "New insights into the photophysics of DNA nucleobases," J. Phys. Chem. Lett. **7**, 4445–4450 (2016).
[77]C. Consani, G. Aubock, F. van Mourik, and M. Chergui, "Ultrafast tryptophan-to-heme electron transfer in myoglobins revealed by UV 2D spectroscopy," Science **339**, 1586 (2013).

[78]N. Krebs, I. Pugliesi, J. Hauer, and E. Riedle, "Two-dimensional Fourier transform spectroscopy in the ultraviolet with sub-20 fs pump pulses and 250–720 nm supercontinuum probe," New J. Phys. **15**, 085016 (2013).
[79]R. B. Varillas *et al.*, "Microjoule-level, tunable sub-10 fs UV pulses by broadband sum-frequency generation," Opt. Lett. **39**, 3849–3852 (2014).
[80]I. V. Rubtsov, J. Wang, and R. M. Hochstrasser, "Dual frequency 2D-IR of peptide amide-A and amide-I modes," J. Chem. Phys. **118**, 7733–7736 (2003).
[81]D. V. Kurochkin, S. R. G. Naraharisetty, and I. V. Rubtsov, "Dual-frequency 2D IR on interaction of weak and strong IR modes," J. Phys. Chem. A **109**, 10799–10802 (2005).
[82]H. Seiler, S. Palato, B. E. Schmidt, and P. Kambhampati, "Simple fiberbased solution for coherent multidimensional spectroscopy in the visible regime," Opt. Lett. **42**, 643–646 (2017).
[83]M. Kullmann, S. Ruetzel, J. Buback, P. Nuernberger, and T. Brixner, "Reaction dynamics of a molecular switch unveiled by coherent two-dimensional electronic spectroscopy," J. Am. Chem. Soc. **133**, 13074–13080 (2011).
[84]N. M. Kearns, R. D. Mehlenbacher, A. C. Jones, and M. T. Zanni, "Broadband 2D electronic spectrometer using white light and pulse shaping: Noise and signal evaluation at 1 and 100 kHz," Opt. Express **25**, 7869–7883 (2017).
[85]D. Zhong, "Electron transfer mechanisms of DNA repair by photolyase," Annu. Rev. Phys. Chem. **66**, 691–715 (2015).
[86]R. F. Pauszek, G. Kodali, M. S. U. Siddiqui, and R. J. Stanley, "Overlapping electronic states with nearly parallel transition dipole moments in reduced anionic flavin can distort photobiological dynamics," J. Am. Chem. Soc. **138**, 14880–14889 (2016).
[87]J. Brazard *et al.*, "New insights into the ultrafast photophysics of oxidized and reduced FAD in solution," J. Phys. Chem. A **115**, 3251–3262 (2011).
[88]D. Q. Xiao, S. S. Skourtis, I. V. Rubtsov, and D. N. Beratan, "Turning charge transfer on and off in a molecular interferometer with vibronic pathways," Nano Lett. **9**, 1818–1823 (2009).
[89]M. Fedoseeva, M. Delor, S. C. Parker, I. V. Sazanovich, M. Towrie, A. W. Parker, and J. A. Weinstein, "Vibrational energy transfer dynamics in ruthenium polypyridine transition metal complexes," Phys. Chem. Chem. Phys. **17**, 1688–1696 (2015).
[90]N. Azzaroli, M. G. Lobello, A. Lapini, A. Iagatti, L. Bussotti, M. Di Donato, G. Calogero, M. Pastore, F. De Angelis, and P. Foggi, "Monitoring the intramolecular charge transfer process in the Z907 solar cell sensitizer: A transient vis and IR spectroscopy and *ab initio* investigation," Phys. Chem. Chem. Phys. **17**, 21594–21604 (2015).
[91]R. Osterbacka, C. P. An, X. M. Jiang, and Z. V. Vardeny, "Two-dimensional electronic excitations in self-assembled conjugated polymer nanocrystals," Science **287**, 839–842 (2000).
[92]R. D. Pensack, K. M. Banyas, L. W. Barbour, M. Hegadorn, and J. B. Asbury, "Ultrafast vibrational spectroscopy of charge-carrier dynamics in organic photovoltaic materials," Phys. Chem. Chem. Phys. **11**, 2575–2591 (2009).
[93]L. W. Barbour, M. Hegadorn, and J. B. Asbury, "Watching electrons move in real time: Ultrafast infrared spectroscopy of a polymer blend photovoltaic material," J. Am. Chem. Soc. **129**, 15884–15894 (2007).
[94]A. A. Bakulin *et al.*, "Charge-transfer state dynamics following hole and electron transfer in organic photovoltaic devices," J. Phys. Chem. Lett. **4**, 209–215 (2013).
[95]Y. Vaynzof, A. A. Bakulin, S. Gelinas, and R. H. Friend, "Direct observation of photoinduced bound charge-pair states at an organic-inorganic,", " semiconductor interface," Phys. Rev. Lett. **108**, 246605 (2012).
[96]S. D. Dimitrov *et al.*, "On the energetic dependence of charge separation in low-band-gap polymer/fullerene blends," J. Am. Chem. Soc. **134**, 18189–18192 (2012).
[97]A. A. Bakulin *et al.*, "The role of driving energy and delocalized states for charge separation in organic semiconductors," Science **335**, 1340–1344 (2012).